1   When the MOUSE leaves the house

2   Bernhard Blümich[1], Jens Anders[2]

3   [1]Independent researcher, 52159 Roetgen, Germany
4   [2]Institute of Smart Sensors, University of Stuttgart, 70569 Stuttgart, Germany

5   Correspondence to: Bernhard Blümich (bluemich@rwth-aachen.de)

6   **Abstract.** Change is inherent to time being transient. With the NMR-MOUSE having matured into an established
7   NMR tool for nondestructive testing of materials, this forward-looking retrospective assesses the challenges the
8   NMR-MOUSE faced when deployed outside a protected laboratory and how it's performance quality can be
9   maintained and improved when operated under adverse conditions in foreign environments. This work is dedicated
10   to my dear colleague and friend Geoffrey Bodenhausen on the occasion of his crossing an honorable timeline in
11   appreciation of his ever-continuing success of fueling the dynamics of magnetic resonance.

12   **1. Introduction**

13   The MOUSE (MObile Universal Surface Explorer) (Eidmann et al., 1996) is a portable stray-field NMR sensor
14   suited for non-destructive testing of materials (Blümich et al., 2008; Casanova et al., 2011) With it the relaxation
15   of nuclear spins towards equilibrium is measured following perturbation by radio-frequency pulses. The sensor is
16   a small and compact NMR relaxometer that investigates an object from one side and can be carried along to the
17   site of interest. As such the NMR-MOUSE and other stray field relaxometers are one modality of compact NMR.
18   Other modalities are tabletop relaxometers, tabletop imagers and tabletop spectrometers (Blümich et al., 2014;
19   Blümich, 2016; Blümich and Singh, 2018).

20   While the size of most NMR instruments today is dominated by a large superconducting magnet, compact
21   NMR relaxometers have small permanent magnets. They were commercially introduced in the early 1970ies to
22   assist the food industry in characterizing emulsions (van Putte and van den Enden, 1974; Blümich, 2019). Today
23   tabletop relaxometers are employed to study a wide range of materials, in particular, foodstuffs, polymers, and
24   porous media (Blümich et al., 2014; Blümich, 2016; Blümich and Singh, 2018; Saalwächter, 2012). A key feature
25   of these early tabletop instruments is that samples need to be drawn and inserted into the hole in the magnet for
26   analysis. In this respect, the measurement is destructive. This equally applies to modern tabletop NMR
27   spectrometers for chemical analysis unless they are operated in flow-through mode, like in a process control
28   environment (Kern et al., 2019). While NMR spectrometers with permanent magnets were built already in the
29   early 1950s (Gutowski, 1953; Blümich, 2019), their magnets were large and could produce only a small field
30   region sufficiently homogeneous to resolve the proton chemical shift. Small permanent magnets with
31   homogeneous fields are challenging to build due to the variations in dimensions, polarization magnitude, and
32   direction of the magnet elements. Therefore, the routine use of compact NMR instruments remained limited for a
33   long time to relaxation and diffusion measurements until the technology of compact high-resolution magnets had
34   been sufficiently advanced about ten years ago (Danieli et al., 2010; Blümich, 2016; Blümich and Singh, 2018).
35   Before that, chemical analysis with tabletop instruments was explored primarily by a few dedicated research
36   groups (Nordon et al., 2001; Dalitz et al., 2012).

37   Mobile NMR instruments need to be both compact and robust to deploy them at different sites and in
38   different environments. The era of mobile NMR began with well-logging instruments shortly after the first NMR
39   experiments in condensed matter in December 1945. Already in 1952, Russel Varian patented a subsurface well
40   logging method and apparatus (Varian, 1952; Woessner, 2001). The sensor to be inserted into the borehole of an
41   oil-well and operating in the earth's magnetic field eventually evolved into tube-shaped instruments housing
42   permanent magnets as well as transmit and receive electronics to analyze the relaxation of ^{1}H NMR signals from
43   particular regions localized in the borehole wall (Jackson et al., 1980; Kleinberg and Jackson, 2001). In his
44   introduction to the 2016 book "Mobile NMR and MRI" (Johns et al., 2016), Eiichi Fukushima reviews the
45   evolution of earth-field and mobile NMR with particular attention to these early developments (Fukushima, 2016).
46   Well-logging NMR is also known as inside-out NMR because the instrument is inserted into the object and
47   not the object into the magnet. Inside-out NMR is mobile but also destructive, as a hole needs to be drilled into the
48   object (Jackson et al., 1980, Coates et al., 1999). The underlying concept of mobile stray-field relaxometry was
49   extended at the Southwest Research Institute, San Antonio, Texas, to nondestructive materials testing with NMR
50   relaxometers accessing the object from one side. These instruments were already transportable, whereby some of
51   them using bulky and massive electromagnets, others more compact permanent magnets (Fukushima, 2016). The
52   magnets were laid out to maximize the field volume containing the spins which can be excited selectively from
53   within the bulk with rf pulses in an effort to maximize the hydrogen signal from the object of interest next to the
54   sensor deriving from moisture in soil, bridge decks, building structures, and food products (Fukushima, 2016;
55   Blümich et al., 2008; Blümich, 2016; Blümich, 2019). Within this volume the field gradient must be small so that
56   the resonance frequencies of the spins inside are within the bandwidth of the rf excitation pulses. As a consequence,
57   the field strength was low.
58   One may argue that the era of mobile NMR with compact sensors essentially started with the appearance
59   of the NMR-MOUSE, a stray-field relaxometer that in its design disregarded the quest for a large sensitive volume
60   by fortuitous ignorance (Eidmann et al., 1996). The small sensor exhibits a large field gradient, and consequently
61   a small sensitive volume yet a strong stray field. Compared to larger sensors the opposing impacts on the sensitivity
62   of a smaller signal-bearing volume and higher field strength turned out to largely balance each other so that at
63   comparable sensitivity the more compact sensors (Blümich et al., 2008) were easier to carry along and be moved
64   from one place to another than other stray-field sensors.

65   **2. The NMR-MOUSE in the house**

66   While brainstorming the simplest realization of NMR in 1993 at the Max-Planck Institute for Polymer Research
67   in Mainz, Peter Blümler asked the question: "Would it not be nice to have an NMR scanner that one moves across
68   the surface of an object to look inside just like an ultrasound scanner?" (Armstrong-Smith, 2015). The next day he
69   came with a drawing how such a device could look like, and we dubbed it NMR-MOUSE for 'MObile Universal
70   Surface Explorer'. Having taken up the Chair of Macromolecular Chemistry at RWTH Aachen University the
71   same year, the realization of the NMR-MOUSE was the project of Blümich's first PhD student Gunnar Eidmann,
72   who succeeded to get the first signal in 1995 (Eidmann et al., 1996). Hardware improvements, measurement
73   methodology and applications of the NMR-MOUSE were systematically explored over the years in particular by
74   Peter Blümler, Gisela Guthausen, Sophia Anferova, Valdimir Anferov, Federico Casanova and Juan Perlo. The
75   NMR-MOUSE has found numerous applications for nondestructive materials characterization by relaxation and

76 diffusion measurements (Blümich et al., 2008; Casanova et al., 2011). The design of many early stray-field

77 relaxometers and of the original NMR-MOUSE was that of a simple u-shaped magnet. It is marketed by Bruker

78 under the name 'minispec ProFiler'. This sensor has a roughly cup-shaped sensitive volume, the position, and

79 shape of which are defined by the profiles of the stray fields produced by the permanent magnet and the radio-

80 frequency coil (Eidmann et al., 1996, Hürlimann and Griffin, 2000; Balibanu et al., 2000).

81   A major improvement of the original sensor was to shim the sensitive volume from bowl-shape to a flat

82 with a slice diameter of about 10 mm, and, depending on the measurement scheme, a slice width less than 3 μm

83 (Perlo et al., 2005), enabling the acquisition of high-resolution depth profiles by translating the sensor in-between

84 measurements with high precision. To this end, two u-shaped or horseshoe magnets are placed side by side with a

85 small gap (Fig. 1a, bottom). The measurement principle followed to acquire depth profiles is the same as that

86 employed for logging oil wells except that the NMR-MOUSE sensor is horizontally moved between consecutive

87 measurements in steps on the order of 0.1 mm instead acquiring NMR signal while the well-logging tool is moving

88 laterally with respect to the magnet surface for distances on the order meters. Today, the NMR-MOUSE for high-

89 resolution depth profiling is a heritage product of Magritek GmbH with its production site in Aachen, that is

90 managed by the two NMR-MOUSE pioneers Federico Casanova and Juan Perlo. In fact, Magritek today is the

91 result of a 2012 merger of Magritek Ltd. from New Zealand, which, among others, developed the Kea spectrometer

92 motivated by Paul Callaghan's Antarctic expeditions (Callaghan et al., 1998), and ACT GmbH, a company spun

93 off from RWTH Aachen University, which produced the Profile NMR-MOUSE.

94
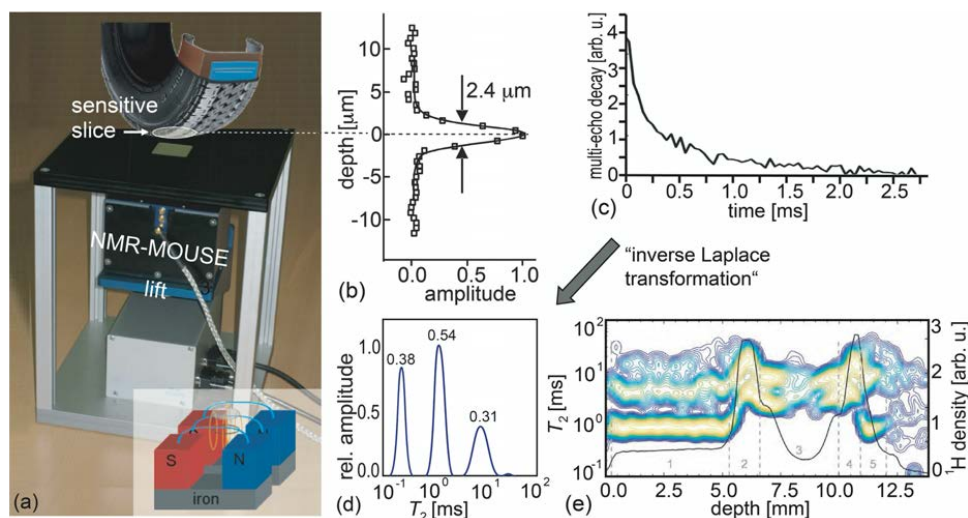
96 Figure 1. The principle of measuring depth profiles with the Profile NMR-MOUSE. a) Conceptual picture of the
97 profile NMR-MOUSE on a lift with its sensitive slice inside a rubber tire. b) Point-spread function of the record
98 depth resolution. c) Experimental signal decay measured with a multi-echo train. d) Distribution of relaxation
99 times from tire-tread rubber derived by inversion of a signal decay with an algorithm, referred to as "inverse
100 Laplace transformation". e) Collection of distributions of relaxation times and signal amplitudes reporting nominal
101 spin density measured across a range of 14 mm into a tire tread.

102

103   To measure depth profiles, the sensor is mounted on a precision displacement stage with which the sensitive

104 slice at a fixed distance from the magnet surface can be moved through the object step by step between acquisitions

105 of multi-echo trains and more advanced two-dimensional Laplace methods (Blümich et al., 2014). The envelope

106 of a multi-echo train provides a stroboscopically sampled transverse relaxation decay (Fig. 1c) from which a depth-

107 profile amplitude can be derived in different ways to provide NMR parameter contrast based the relaxation-time

108 distribution (Fig. 1d), the hydrogen density corresponding to the signal amplitude from the spins in the sensitive

109 slice (Fig. 1e), relaxation times, and molecular self-diffusion (Blümich et al., 2008; Casanova et al., 2011; Blümich

110 et al., 2014).The signal amplitude is the full integral of the relaxation-time distribution. Partial integrals of

111 individual peaks provide component concentrations. To assign physical meaning to individual peaks is not as

112 straight forward as interpreting the chemical shift of resonance lines in a high-resolution NMR spectrum. Yet the

113 peak amplitudes and positions vary with material properties (Fig. 1e), and it often takes the treasure of experience

114 or a reference data base to interpret distributions of relaxation times for practical applications.

115

116

117 Figure 2. The evolution of stray-field NMR at RWTH Aachen University. a) The original NMR-MOUSE
118 measuring a car tire. b) An early version of the NMR-MOUSE with copper-shielded magnets for dead-time
119 reduction. c) The original NMR-MOUSE in 2000. d) The bar-magnet NMR-MOUSE is the simplest construction
120 of a stray-field NMR sensor. e) In 2003 Juan Perlo developed the smallest tomograph in stray-field technology
121 (Foto: Peter Winandy). f) A single-sided tomograph with a flat imaging plane. Right: Set-up for mapping a tire
122 tread. Left: A photo (top) in comparison with an MR image (bottom). g) The Profile NMR-MOUSE with a flat
123 sensitive slice developed in 2005. h) Stray-field NMR magnet capable of measuring chemical-shift resolved ^{1}H
124 NMR spectra from a fluid in a beaker placed on top of the magnet. i) Fourier NMR-MOUSE with shim magnets
125 producing a 2 mm thick sensitive slice for frequency encoding of depth. j) Mini-MOUSE with a multi-layered
126 micro-coil having a dead-time of 10 μs. k) Micro-MOUSE constructed from four 1 cm^3 permanent magnet cubes.
127

128 The hardware, use, and measurement methodology of the NMR-MOUSE has been studied for more than

129 two decades in various research projects at RWTH Aachen University and other places. Its use for testing different

130 materials such as rubber, polymers, building materials, food, and objects of cultural heritage is reported in books

131 and reviews (Blümich, 2000; Blümich, 2008; Blümich et al., 2008; Blümich et al., 2010; Casanova et al., 2011;

132 Capitani et al., 2012; Blümich et al., 2014, Baias and Blümich, 2017; Capitani et al., 2017, Blümich, 2019; Rehorn

133 and Blümich, 2018; Blümich, 2019). Several modifications of the original NMR-MOUSE in addition to the

134   forerunner of the current Magritek Profile NMR-MOUSE (Fig. 1a) have been investigated at RWTH Aachen

135   University. Recognizing that the information content extractable from the signal of the sensitive region in stray-

136   field NMR corresponds to that accessible in a voxel of a magnetic resonance image, first applications of the NMR-

137   MOUSE were explored with car tires representing soft synthetic matter (Fig. 2a) in line with the main use of MRI

138   in imaging soft biological matter. The horseshoe set-up (Fig. 2b) was subsequently made smaller and packed in a

139   more attractive shell (Fig. 2c). Realizing that the horse-shoe magnet having the B_0 stray field essentially parallel

140   to its active surface could further be simplified, the bar-magnet NMR-MOUSE was built from a magnet block first

141   cuboid-shaped (Blümich et al., 2002) and later cylinder-shaped with B_0 perpendicular to the active end face and a

142   figure-eight rf coil with B_1 parallel to it (Fig. 2d). The maximum depth of access is lower than for the horseshoe

143   sensor, but the deadtime is shorter due to the gradiometer property of the rf coil (Anferova et al., 2002). Note that

144   contrary to the B_0 orientation perpendicular to the active surface, B_0 parallel to the active surface enables studying

145   macroscopic molecular order in anisotropic materials such as tendon and strained rubber (Haken and Blümich,

146   2000; Hailu et al, 2002.

147   While improving the original NMR-MOUSE, also a single-sided tomograph was developed and tested in

148   the DFG-funded Collaborative Research Center on Surface NMR of Elastomers and Biological Tissue FOR333.

149   One result from this project was the smallest MRI instrument at the time obtained by fitting a bar-magnet NMR-

150   MOUSE with coils for pulsed gradient fields (Fig. 2e) (Casanova and Blümich, 2003). Another result was an

151   improved u-shaped magnet with thicker ends at each side of the poles so that the magnet assembly produced a flat

152   imaging plane (Fig. 2f) (Casanova and Blümich, 2003; Blümich et al., 2005). Images from a plane parallel to the

153   sensor surface could be measured with pure phase encoding schemes, but the sensitivity was low due to the thin

154   slice resulting from a strong stray-field gradient. Maintaining the flat sensitive region of the imaging plane, this

155   complex magnet geometry was subsequently simplified to two u-shaped magnets placed at a specific distance next

156   to each other, resulting in the Profile NMR-MOUSE (Fig. 1a, Fig. 2g), which proved to be a robust stray-field

157   NMR sensor constructed from a minimum number of parts (Perlo et al., 2005).

158   Flattening the sensitive region of a stray-field magnet to a plane was a milestone in understanding how to

159   shim the stray field. Eventually, the sensitive region in the stray field could be homogenized locally with the help

160   of additional shim magnets to a degree sufficient to resolve the ^{1}H chemical shift from a limited volume of fluid

161   inside a beaker on top of the magnet (Fig. 2h) (2014; Perlo et al., 2005; Perlo et al., 2006; Zalesskiy et al.). Another

162   advance was the construction of a stray-field sensor with a sensitive slice having a homogeneous gradient field in

163   the sensitive slice across an extended depth range of 2 mm for single-shot depth profiling by frequency encoding

164   of position (Fig. 2i) (Van Landeghem et al., 2012). With this sensor the time to acquire a depth profile into soft

165   matter was reduced considerably, and it proved useful for *in vivo* applications like mapping human skin [46] and

166   monitoring perfusion states of the small intestine by diffusion maps (Krechenau et al., 2018).

167   The NMR-MOUSE has also been miniaturized and fitted with multi-layered micro-coils (Fig. 2j,k)

168   (Oligschläger et al., 2014; Oligschläger, Kupferschläger, et al. 2015), by which, on the expense of 7.6-fold lower

169   sensitivity compared to the PM5 NMR-MOUSE at 1 mm access depth, the dead time of the measurement could

170   be reduced to a record 10 µs echo time. With its small coil, the signal from the cement regions between the stone

171   aggregate in cuts of concrete could be focused on, and with an echo time ≤ 20 µs the hitherto hidden signals from

172   bound water in the dry grey cement could be measured (Fig. 3a) (Oligschläger, Kupferschläger, et al. 2015). At

173   the same echo time, even the rapidly relaxing transverse magnetization from the crystalline domains of

174   polyethylene was detectable (Fig. 3b). The presence of the rapidly decaying signal components at $t_E = 20$ µs nearly

175 doubles the amplitude of the recorded magnetization decays compared to the amplitudes recorded with the
176 minimum echo time of 70 μs of the reference laboratory NMR-MOUSE with 10 mm depth of access. As the short
177 dead time of the mini-MOUSE had been achieved at the cost of a small sensitive volume and a low depth of access
178 due to the small diameter of the coil, it is the ambition of current sensor improvement to reduce the deadtime at
179 coil diameters 10 mm and more. Currently, for example, the minimum echo time of the Magritek PM25 NMR-
180 MOUSE is 50 μs when fitted with spacers and a 15 mm diameter coil to limit the depth of access to 10 mm. For a
181 new PM2 NMR-MOUSE with 2 mm depth of access the minimum echo time of the is just 15 μs. Even shorter
182 echo times may eventually be realized with novel transceiver circuits that promise the detection of the spin
183 response during the rf pulse (Anders, 2020). Moreover, to shorten the acquisition time from hours to minutes for
184 field applications like investigations of glass- or carbon-fiber reinforced polymer materials employed in windmill
185 wings and airplane rudders, the detection of the bitumen component in asphalt (Blümich et al., 2019) and the bound
186 water in cement, a large sensitive volume is needed. This can be achieved, for example, with a coil array
187 (Oligschläger, Lehmkuhl, et al. 2015) [53] placed on a suitably tailored magnet surface (Blümich et al., 1999).

188
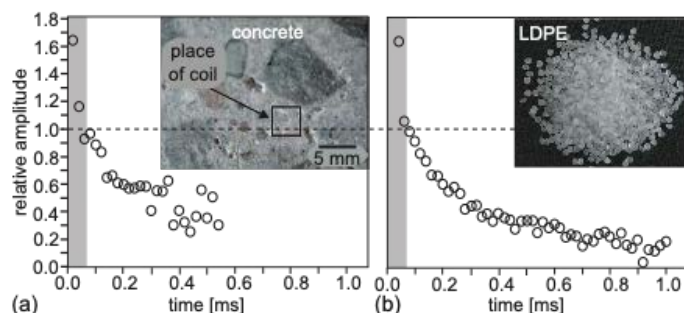
189
190 Figure 3. Transverse magnetization decays acquired with the Mini-MOUSE (Fig. 2j) at short echo time t_E. The
191 shaded area marks signal lost at a deadtime of 70 μs. a) The signal from bound water in dry, grey cement. b) The
192 crystalline protons in low-density polyethylene with $T_2 = 12$ μs can be detected at $t_E = 20$ μs.

193 **3. The NMR-MOUSE outside the house**

194 The NMR-MOUSE was introduced to the cultural heritage community through the effort of Annalaura Segre at
195 the turn of the millennium (Segre and Blümich, 2002), and from 1999 to 2019 its further refinement has benefitted
196 greatly from the cultural heritage projects EUREKA-Eurocare Σ!2212-MOUSE, EU-ARTECH, CHARISMA, and
197 IPERION-CH. With the exception of well-logging relaxometry (Coates et al, 1999), it is common practice to
198 conduct NMR measurements in a laboratory. But objects of cultural heritage often cannot leave the museum or
199 are immobilized, e. g. at excavation sites, so that the NMR-MOUSE has to be moved to the site and operated under
200 the prevailing environmental and climatic conditions. These can be rather challenging at times for the operators as
201 well as for the equipment, which has been designed primarily for indoor use.
202   For some outdoor applications like determining the crumb-rubber content in asphalt pavements (Blümich
203 et al., 2019), depth profiling is not essential. But for others it is crucial. This includes the analysis of easel paintings
204 (Presciutti et al., 2008; Fife et al., 2015; Angelova et al., 2016; Prati et al., 2019; Busse et al., 2020), frescoes
205 (Rehorn et al., 2018), and mummies (Rühli et al., 2007; Blümich et al., 2014). A less obvious application is the
206 analysis of moisture distributions, for example, in walls. Moisture maps with crude lateral resolution and high

207   depth resolution can assist in locating a moisture leak (Proietti et al., 2007; Rehorn and Blümich, 2018; Blümich,
208   2019; Blümich in Bastidas and Cano, 2019). Although time consuming, high-resolution depth profiles of
209   volumetric, quantitative moisture content are more significant than the volume-averaged numbers delivered by
210   most methods other than the NMR-MOUSE including evanescent field dielectrometry (Olmi et al., 2006). The
211   latter method derives moisture content and the presence of salt from the dielectric properties of a wall exposed to
212   an electric field with a frequency of about 1 GHz. The electric wave enters the wall up to about 20 mm, so that the
213   delivered moisture content is a weighted volume average across that depth range. While the measurement is fast,
214   the depth resolution is inadequate for further analysis, because the moisture content varies significantly over the
215   20 mm as demonstrated with measurements of wall moisture in the Chapel of St. Mary of the Abbeye de Chaalis
216   (Fig. 4). Volumetric moisture content is easy to quantify at short echo time, by simply taking the signal amplitude
217   from a particular spot inside the wall and normalizing it to the amplitude of the signal from pure water measured
218   with the same instrumental parameter settings.

219
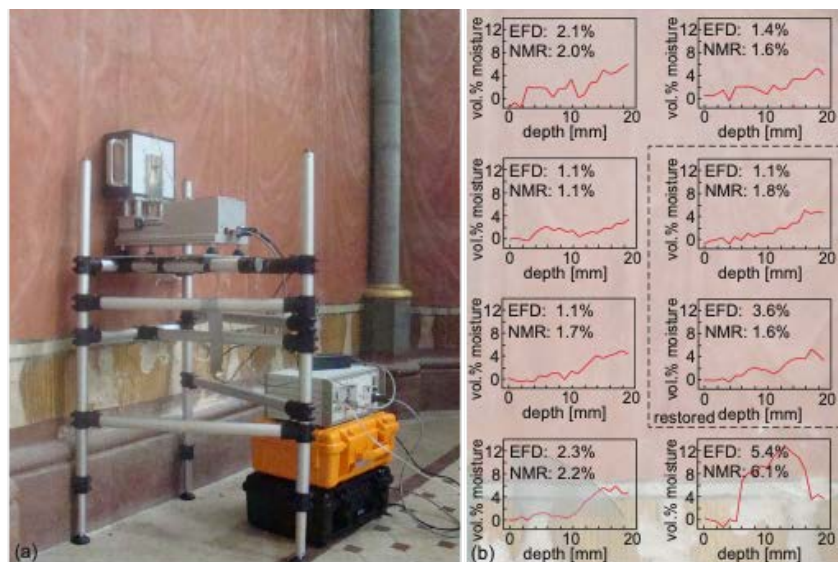
220
221   Figure 4. Moisture measurements at the painted wall left of the altar inside the Chapel of St. Mary in Chaalis. a)
222   Set-up for NMR depth profiling. b) High-resolution depth profiles from eight positions. The moisture-content
223   values from evanescent field dielectrometry (EFD) are compared to NMR values derived from integration of
224   quantitative moisture depth profiles weighted with the heuristic depth attenuation function, which is indicated by
225   the shaded region in the bottom left profile.
226

227   The measurement conditions encountered in historic buildings and outdoors are often challenging to meet
228   with equipment designed for laboratory use (Fig. 5). Examples are the presence of water, rain or steam (Fig.
229   5a,g,h), passing cars (Fig. 5b,c), testing spots a few meters high (Fig. 5d,e), and treasures of outstanding value
230   inside a guarded museum laboratory (Fig. 5f). The climate conditions can range from hot, e.g., up to 38° C air
231   temperature (Fig. 5c) and close to boiling water temperature (Fig. 5h) to cold, e.g. down to 5° C (Fig. 5a). The
232   environment may be dusty with magnetic sand particles or wet from streaming rain (Fig. 5g). In many cases, a
233   power grid can be accessed, but in some cases, the equipment needs to be operated from a battery (Fig. 6h) or an
234   electric power generator. Apart from the power supply, different units need to be connected with several cables at

235 the site. These units are an NMR-MOUSE with 10 mm or 25 mm depth range, a precision translational stage, a
236 fragile spectrometer console, and a laptop computer. The electrical connectors can break during transport and
237 assembly. The connecting cables often form ground loops that produce 50/60 Hz hum and pick up environmental
238 electromagnetic noise. However, the latter can successfully be shielded in most cases with the help of silver-coated
239 and electrically grounded parachute silk (Fig. 5g) or rabbit fence. Moreover, a stable scaffold finely adjustable in
240 height and suitable to be set up on uneven ground is needed to accurately position the NMR-MOUSE at the spot
241 of interest (Fig. 4a). All these parts along with basic tools for emergency repair are usually packed into plastic
242 transportation boxes and shipped to the site of interest prior to the measurement campaign.

243
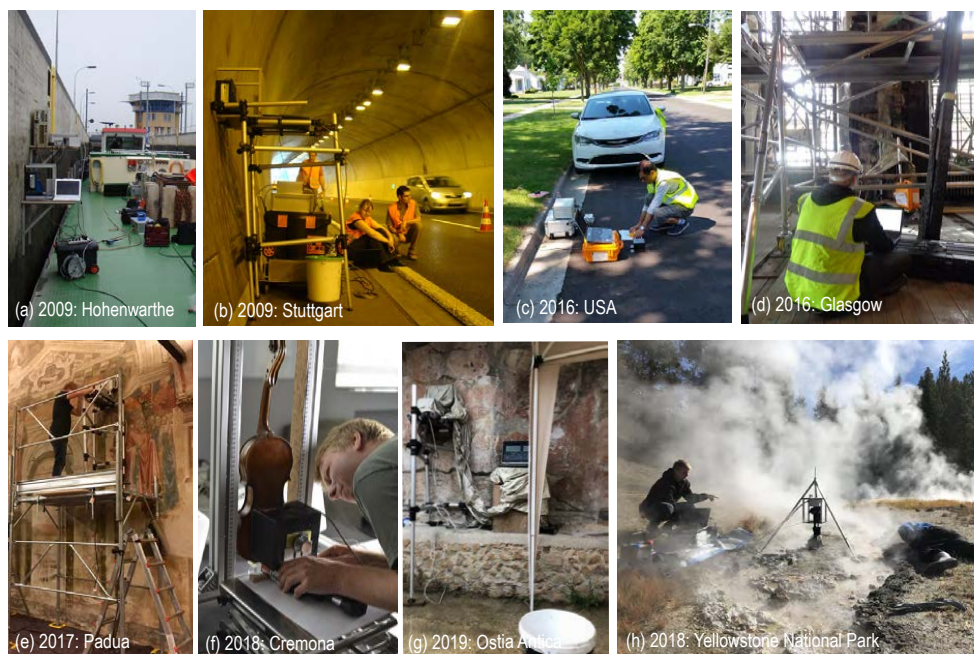
244

245 Figure 5. The MOUSE outside the house. a) Profiling the moisture content of the grey concrete wall of the lock
246 Hohenwarthe. b) Profiling moisture in the concrete wall of the Gäubahn tunnel near Stuttgart. c) Analyzing the
247 crumb-rubber content in asphalt pavement (Foto: Yadoallah Teymouri). d) Assessing the fire damage of sandstone
248 in the Mackintosh library of Glasgow. e) Searching for a hidden Giotto fresco in Padua. f) Measuring a depth
249 profile though the back of a Stradivari violin in Cremona. g) In search for a hidden wall painting in Ostia Antica
250 on a rainy day. h) Profiling sediment-covered biofilms at the hot springs in Yellowstone National Park.

251

252 A practical point of concern in measuring high-resolution depth profiles is the proper placement of the
253 sensitive slice parallel to the stratigraphy of the object. Assuming that the sensitive slice is 10 mm wide and 0.1
254 mm thick, the misalignment angle between the plane of the slice and the layers to be resolved needs to be smaller
255 than one degree (Blümich et al., 2020). With a laboratory setup, the sensitive slice and the object surface can be
256 accurately aligned when the NMR-MOUSE is properly placed on the sample table of the lift to which the sensitive
257 slice had been aligned by the manufacturer (Fig. 1a). But measurements in the field usually employ a translation
258 stage without a sample table (Figs. 4a, 5f, 5h) so that the sensor is aligned with the object surface by eye. Moreover,
259 the minimum distance between the sensor and the object needs to be as small as possible, i. e. 1 mm or less, at the
260 start of profiling in order to maximize the depth range into the object. Setting alignment and minimum distance is

261   a critical part of the experiment setup. Electronic guidance for both would greatly simplify the setup procedure

262   and improve the reproducibility of measurement.

263   **4. Improving the fitness of the NMR-MOUSE for adventures outside the house**

264   It is the accumulated experience with cultural heritage studies, which suggests a number of improvements to bring

265   the NMR-MOUSE in shape for the adventures encountered when leaving the house and operating outdoors. These

266   are:

267   1)   Combine all electronics into one instrument comprising the translation stage, the NMR-MOUSE and the

268   transmit-receive electronics.

269   2)   Incorporate distance and alignment sensors into the instrument.

270   3)   Employ a stable sensor scaffold and mounting device that can be assembled quickly at the site and enables

271   measurements at different heights.

272
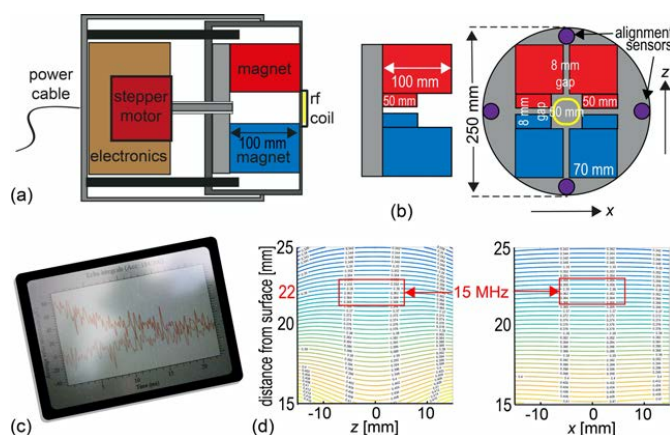
273

274   Figure 6. Concept of an all-in-one NMR-MOUSE for depth profiling. a) Axial cross section through two telescoped
275   tubes showing the stepper motor along with the transmit-receive electronics on the left in the outer tube and the
276   NMR-MOUSE on the right in the inner tube. b) Arrangement of magnets and alignment sensors. c) The instrument
277   should be controlled via WLAN or Bluetooth. d) Calculated field map predicting the position of the sensitive slice
278   at 22 mm above the magnet surface.

279   **4.1 The all-in-one instrument**

280   The envisioned all-in-one NMR-MOUSE for depth profiling outdoors would have a minimum number of

281   components connected by cables (Fig. 6). The components need to be small for ease of transportation and rugged

282   for operation outdoors. The power supply would be either a 12 V car battery or a power supply that connects to

283   the grid or an electric generator. It hooks up to the NMR instruments (Fig. 6a) with the only cable of the setup.

284   The instrument comprises the translation stage, the transmit-receive electronics, and the magnet (Fig. 6b). It would

285   be operated in wireless mode via WLAN or Bluetooth from a tablet personal computer (Fig. 6c), so that it can be

286   set up on tall scaffolds (Fig. 5e), and long measurements could be controlled and monitored from the distance

287   including the hotel room at night.

288   Assuming a 250 mm inner diameter tube, a computer simulation suggests that a Profile NMR-MOUSE

289   magnet configuration would produce a sensitive slice 22 mm above the magnet surface (Fig. 6d) with a field

strength corresponding to a 15 MHz ^{1}H resonance frequency. Subtracting the space for the coil and the case, the resultant depth of access would be 15 mm, which is a reasonable working depth for many applications ranging from easel paintings to violins and frescoes. The magnets would be mounted in the inner of two telescoped tubes, which can slide in and out of the outer one under control of a precision stepper motor. The outer tube would house the stepper motor and the transmit-receive electronics and be attached to the mounting gear for depth profiling. The total length of the pipe assembly would be shorter than 300 mm.

Commercial tabletop NMR instruments employ compact transmit-receive electronics (Blümich et al., 2014; Blümich, 2016; Blümich and Singh, 2018), which, although reliable, nevertheless, are too large and power-hungry for mobile use. Their state-of-the-art has been surpassed by the development of smaller, single-chip based magnetic resonance transceivers (Zalesskiy et al., 2014; Ha et al., 2014; Ha et al., 2015; Grisi et al., 2015; Chu et al., 2017; Anders et al., 2017). In particular, a small monolithic spectrometer has been developed (Bürkle et al., 2020), which uses a high-voltage CMOS process with supply voltages up to 25 V for enhanced driving strength to combine the monolithic NMR-on-a-chip approach with macroscopic, cm-sized coils. This approach promises a 90°-pulse width of 5 μs for an echo time of 20 μs at a depth of access of 10 mm, rendering high-voltage NMR-on-a-chip transceivers well suited for use in a compact all-in-one NMR-MOUSE sensor.

4.2 Distance and alignment sensors

The implementation of distance and alignment sensors is a highly needed improvement over the current state-of-the-art, where the NMR sensor has to be aligned visually parallel to the object as close as 0.5 mm (Blümich et al., 2020). The misalignment angle of the sensitive slice with the parallel layer structures of the object needs to be less than one degree if the spatial resolution is to be better than 200 μm. But visual alignment parallel to an extended surface is hardly possible as one cannot see by eye the narrow gap between the magnet and the surface. Nevertheless, in practice, object and sensor have usually been aligned visually (Fig. 5f,h) with surprisingly good results in most cases but only fair reproducibility even for expert users. To enable the required reproducibility, alignment sensors need to be incorporated with the help of which the sensitive plane can be accurately aligned with the object at a fixed distance. Once aligned at a known distance, the sensor can be advanced or retracted to its starting position with the stepper motor.
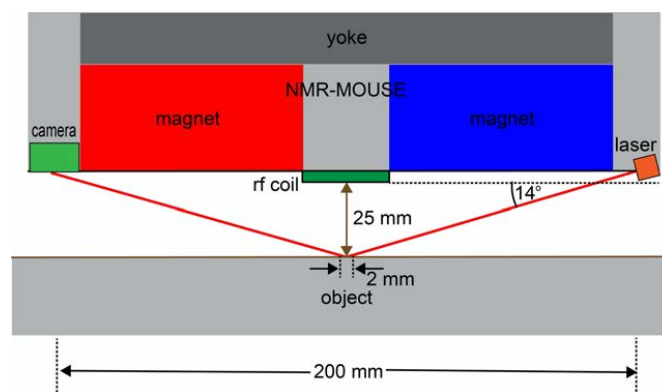
Figure 7. Concept of distance sensing with a laser beam at shallow incidence. If the alignment angle of the reflecting plane changes by 0.2°, the reflected laser beam is displaced from the center of the detector camera by 4 mm.

321

322   Elements for alignment-sensor components can be mounted in the four spaces of the inner tube delineated
323 by the tube's inner surface and the secants defined by the outer magnet surfaces (Fig. 5b). Different sensing
324 principles can be considered. The surface spot to align the sensor with the object needs to be at least one millimeter
325 wide to average effects of surface roughness. Therefore, ultrasonic distance sensors appear to be more suitable
326 than regular laser-point distance sensors with spot widths of 10 mm vs. 70 μm, respectively. Yet commercial
327 ultrasonic sensors measure distances within a 25 mm range with 0.75 mm reproducibility, which is an order of
328 magnitude short of the required alignment accuracy if the sensors are 200 mm apart. Therefore, a better option are
329 distance sensors built from lasers with a shallow angle of incidence of 14°, which illuminate a 2 mm diameter spot
330 in the center underneath the coil at 25 mm distance from the coil surface and receive the reflected light with a
331 camera. A back-of-the-envelope calculation shows that an angle maladjustment of 0.25° will shift the center of the
332 reflected laser beam by 4 mm when laser and detector are 200 mm apart (Figs. 6, 7). This design will provide the
333 needed accuracy and precision for alignment at a fixed distance of 25 mm. Following parallel alignment of
334 sensitive slice and object surface, the gap between sensor and object can be shorted under control of the stepper
335 motor before starting the acquisition of a depth profile by retracting the sensor from the wall in defined steps
336 between measurements.

337 **4.3   Operating software**

338 To operate the equipment at locations with restricted spatial access (Fig. 5e) a wireless control strategy should be
339 followed. The two most important operations to be under remote control are the control of the stepper motor and
340 the data acquisition. A depth profile is typically acquired in two runs. A first profile is acquired at low spatial
341 resolution and signal-to-noise ratio to determine the exact location and depth range of interest. Subsequently, a
342 high-resolution profile is acquired with more scans per spot and smaller step size. Depending on the required
343 information and the time available, either full multi-echo decays are measured for further analysis in terms of
344 distributions of relaxation times, or only the first points of the decays are recorded to determine proton density
345 corresponding, for example, to volumetric moisture content. The measurement progress during depth profiling is
346 usually monitored in regular intervals to catch sporadic noise interference, uninformative data, and erroneous
347 parameter settings as budgeting time is important due to up to two hours long acquisition times for a depth profile
348 and limited access time in museums, historic buildings, and at excavation sites.

349   While operating the NMR-MOUSE appears to be a simple endeavor to most people with a basic
350 understanding of NMR relaxometry or MRI (Blümich et al., 2014; Johns et al., 2016), it is a true barrier to most
351 others interested in using it for materials testing. Therefore, the operating platform should avoid NMR jargon as
352 much as possible and relate the NMR acquisition parameters to object-specific information such as hard, soft, wet,
353 moist, dry, moisture content, component concentration, duration of measurement, etc., which have to be entered
354 by the operator. Prior to measurement, the proper functioning of the equipment needs to be checked, in particular,
355 the noise-level and the phase angle of the transverse magnetization. The proper functioning of the equipment and
356 potential faults should be flagged, and the receiver phase angle be adjusted automatically if needed. Moreover, it
357 should be possible to measure again particular depth ranges identified in previous scans. All raw data need to be
358 saved for later access and processing in expert mode. In addition to the data acquisition, the operating platform
359 needs to include data processing routines, that allow to derive depth profiles with different contrast types from the
360 acquired data, e. g. hydrogen concentration (spin density), relaxation (T_2) weighted spin density (*w*-parameter

361 (Blümich et al., 2014)), peak integrals and peak ratios from distributions of relaxation times, as well as depth-
362 resolved distributions of relaxation times. The latter requires access to an inverse Laplace transform algorithm.
363 Finally, it should be possible to display the data from several measurements at the same scales for comparison and
364 interpretation of results.

365 **4.4 Mounting device and scaffold**

366 Given the dimensions of the magnets (Fig. 6a,b), the weight of the sensor is estimated to approach 40 kg. For depth
367 profiling, the device first needs to be positioned with high accuracy at 0.5 to 1 mm away from the surface of the
368 object, so that depth profiles can be scanned by retracting the sensor between scans in small, preset steps of
369 typically 0.05 to 0.25 mm. This way of scanning assures that the object is not damaged by setting a wrong depth
370 range. The mounting device has to enable manual fine adjustment of the sensor orientation following the readings
371 of the alignment sensors and allow stable positioning of the sensor at various angles with high precision for long
372 times from tens of minutes to a few hours.

373
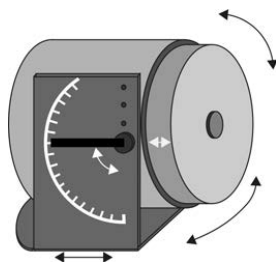
374
375 Figure 8. Conceptual drawing of a sensor mounting device.

376

377 A simple mounting device fulfilling these criteria would consist of a U-shaped aluminum frame (Fig. 8). It
378 would have a flat, felt- or plastic-covered bottom without legs. Position and orientation would be adjusted
379 manually (arrows). To access all polar angles, the polar rotation axis would be adjustable to different values in the
380 device, and one would be able to turn the entire device upside down. To balance the sensor during depth profiling,
381 the horizontal position of the polar rotation axis would be at the average center of gravity for a 20 mm shift range.
382 The bottom plate would be extended at the back to provide a location for clamping the device to a scaffold or table.
383 For most studies outside the lab a modular scaffold had been employed (Fig. 4a), which can be assembled
384 from aluminum tubing with plastic joints in different ways to position the sliding table carrying the NMR-MOUSE
385 at different heights up to about two meters. Each of the three scaffold legs consists of two telescoped tubes so that
386 the legs are extendable via a long, threaded bolts which move the inner tubes in an out by rotating the bolt heads
387 from the top with a cordless electric drill. While this scaffold serves its purpose and is easy to transport and set up,
388 the scaffold is sensitive to vibrations and torsion. Moreover, it would be helpful to be able to adjust its height from
389 the bottom and not the top and with the sensor in place, in particular, when high positions need to be accessed.

390 **5. Summary**

391 Single-sided NMR relaxometry is a technique for nondestructive materials testing. Instruments like the NMR-
392 MOUSE have been developed for use in the laboratory. Applications are found in quality control and aging of

393 polymers and related materials, including PE pipes, PVC flooring, car tires, asphalt pavements, human skin, and
394 food products. The dead time of the current sensors limits the detection of rapidly decaying transverse
395 magnetization, e. g. from bound water in building materials like cement, from glass- and carbon-fiber-reinforced
396 polymer composites in windmill wings, and varnish on paintings and musical instruments. In addition to that, in
397 many cases, measurements need to be conducted at different depths or complete depth profiles need to be acquired.
398 This is the case, e.g., for moisture in walls, where NMR is one if not the only method that directly measures
399 quantitative water content without averaging over depth ranges where the moisture content significantly varies.
400 Emerging applications in cultural heritage studies demand equipment that can easily be transported, set up, and
401 operated. This equipment needs to small and robust. The childhood and adolescence of the NMR-MOUSE
402 equipment have been reviewed and parental advice given for preparation of outdoor measurements and survival
403 outside the protected childhood home.
404

405 **References**

406 Anders, J., Handwerker, J., Ortmanns, M., Boero, G.: A low-power high-sensitivity single-chip receiver for, NMR
407   microscopy, J. Magn. Reson. 266, 41–50, 2017.

408 Anders, J.; Work in progress, 2020.

409 Anferova, S., Anferov, V., Adams, M., et al.: Construction of a NMR-MOUSE with Short Dead Time, Concepts
410   Magn. Reson. B 15, 15–25, 2002.

411 Angelova, L. V., Ormsby, B., Richardson, E.: Diffusion of water from a range of conservation treatment gels into
412   paint films studied by unilateral NMR: Part I: Acrylic emulsion paint, Microchem. J. 124, 311–320, 2016.

413 Armstrong-Smith, I.: A Briefcase Full of NMR, The Analytical Scientist, 26, 24–31, 2015.

414 Baias, M., Blümich, B.: Nondestructive testing of objects from cultural heritage with NMR, in: G.A. Webb,
415   Modern Magnetic Resonance, https://doi.org/10.1007/978-3-319-28275-6_29-1, 2017.

416 Balibanu, F., Hailu, K., Eymael, R., Demco, D. E., Blümich, B.: Nuclear Magnetic Resonance in inhomogeneous
417   fields, J. Magn. Reson. 145, 248–258, 2000.

418 Blümich, B., Anferov, V., Anferova, et al.: Simple NMR-MOUSE with a Bar Magnet, Concepts Magn. Reson.:
419   Magn. Reson. Eng, 15, 155–261, 2002.

420 Blümich, B., Baias, M., Rehorn, C., et al., Comparison of historical violins by non-destructive MRI depth profiling,
421   Microchemical Journal 158, 105219, 2020.

422 Blümich, B., Bruder, M., Guerlin, T., Prado, P.: Device for inspecting flat goods made of polymeric materials with
423   embedded textile strength supports, patent WO200079253A1, 20 June 1999.

424 Blümich, B., Casanova, F., Perlo, J., et al.: Noninvasive testing of art and cultural heritage by mobile NMR, Acc.
425   Chem. Res. 43, 761–770, 2010.

426 Blümich, B., Haber-Pohlmeier, S., Zia, W.: Compact NMR, de Gruyter, Berlin, 2014.

427 Blümich, B., Kölker, C., Casanova, F., Perlo, J., Felder, J.: Ein mobiler und offener Kernspintomograph:
428   Kernspintomographie für Medizin und Materialforschung, Physik in unserer Zeit 36, 236–242, 2005.

429 Blümich, B., Perlo, J., Casanova, F.: Mobile single-sided NMR, Prog. Nucl. Magn. Reson. Spectr. 52, 197–269,
430   2008.

431 Blümich, B., Singh, K.: Desktop NMR and its applications from materials science to organic chemistry, Angew.
432   Chem. Int. Ed. Eng. 57, 6996–7010, 2018.

433 Blümich, B., Teymouri, Y., Clark, R.: NMR on the Road: Non-destructive Characterization of the Crumb-Rubber
434   Fraction in Asphalt, Appl. Magn. Reson. 50 497–509, 2019.

435 Blümich, B.: Concepts and Applications of the NMR-MOUSE, in: Bastidas, D. M., Cano, E.: Advanced
436   Characterization Techniques, Diagnostic Tools and Evaluation Methods in Heritage Science, Springer,
437   Cham, 61–79, 2019.

438 Blümich, B.: Essential NMR for Scientists and Engineers, 2nd ed., Springer, Cham, 2019.

439 Blümich, B.: Low-field and benchtop NMR, J. Magn. Reson. 306, 27–35, 2019.

440 Blümich, B.: Miniature and Tabletop Nuclear Magnetic Resonance Spectrometers, Enc. Anal. Chem. a9458, 1–
441   31, 2016.

442 Blümich, B.: NMR Imaging of Materials, Clarendon Press, Oxford, 2000.

443 Blümich, B.: The Incredible Shrinking Scanner, Scientific American 299, 92–98 2008.

444 Bürkle, H., Schmid, K., Klotz, T., Krapf, R., Anders, J.: A high voltage CMOS transceiver for low-field NMR
445   with a maximum output current of 1.4 A$_{pp}$, 2020 IEEE International Symposium on Circuits and Systems
446   (ISCAS), 10–21 Oct., 10.1109/ISCAS45731.2020.9181025, 2020.

447 Busse, F., Rehorn, C., Küppers, M., et al.: NMR relaxometry of oil paint binders, Magn. Reson. Chem. 58, 830–
448   839, 2020.

449 Callaghan, P. T., Eccles, C. D., Haskell, T. G., Langhorne, P. J., Seymour, J. D.: Earth's Field NMR in Antarctica:
450   A Pulsed Gradient Spin Echo NMR Study of Restricted Diffusion in Sea Ice, J. Magn. Reson. 133, 148–154,
451   1998.

452 Capitani, D., Di Tullio, V., Proietti, N.: Nuclear magnetic resonance to characterize and monitor cultural heritage,
453   Prog. Nucl. Magn. Reson. Spectrosc. 64, 29–69, 2012.

454 Capitani., D., Sobolev, A., Di Tullio, V. D., Mannina, L., Proietti, N.: Portable NMR in food analysis, Chem. Biol.
455   Technol. Agric. 4, 1–14, 2017.

456 Casanova, F., Blümich, B.: Two-dimensional imaging with a single-sided NMR probe, J. Magn. Reson. 163, 38–
457   45, 2003.

458 Casanova, F., Perlo, J., Blümich, B., eds.: Single-Sided NMR, Springer, Berlin, 2011.

459 Chu, A., Schlecker, B., Handwerker, J., et al.: VCO-based ESR-on-a-chip as a tool for low-cost, high-sensitivity
460   food quality control, IEEE Biomedical Circuits and Systems Conference (BioCAS), Turin, 1–4, 2017, doi:
461   10.1109/BIOCAS.2017.8325172, 2017.

462 Coates G. R., Xiao, L., Prammer, L. G.: NMR Logging Principles and Applications, Halliburton, Houston, 1999.

463 Dalitz, F., Cudaj, M., Maiwald, M., Guthausen, G.: Process and reaction monitoring by low-field NMR
464   spectroscopy, Prog. Nucl. Magn. Reson. Spectrosc. 60, 52–70.

465 Danieli, E., Perlo, J., Blümich, B., Casanova, F.: Small magnets for portable NMR spectrometers, Angew. Chem.
466   Int. Ed. 49, 4133–4135, 2010.

467 Eidmann, G., Savelsberg R., Blümler, P., Blümich, B.: The NMR MOUSE, a mobile universal surface explorer,
468   J. Magn. Reson. A122,104–109, 1996.

469 Fife, G. R., Stabik, B., Kelley, A. E., et al.: Characterization of aging and solvent treatments of painted surfaces
470   using single-sided NMR, Magn. Reson. Chem. 53, 58–63, 2015.

471 Fukushima, E.: Introduction, in: Johns, M. L., Fridjohnsson, E. O., Vogt, J. J., Haber, A., eds.: Mobile NMR and
472   MRI: Developments and Applications, Royal. Soc. Chem., Cambridge, 1–10, 2016.

473 Grisi, M., Gualco, G., Boero, G.: A Broadband Single-chip Transceiver for Multi-nuclear NMR Probes, Rev. Sci.
474   Instrum. 86, 044703, 2015.

475 Gutowsky, H. S., Meyer, L.H., McClure, R. E.: Apparatus of Nuclear magnetic Resonance, Rev. Sci. Instrum. 24,
476   644–652, 1953.

477 Ha, D., Paulsen, J., Sun, N., Song, Y.-Q., Ham, D.: Scalable NMR Spectroscopy with Semiconductor Chips, Proc.
478   Nat. Acad. Sci. 111, 11955–11960, 2014.

479 Ha, D., Sun, N., Ham, D.: Next-Generation Multidimensional NMR Spectrometer Based on Semiconductor
480   Technology, eMagRes 4, 117–126, 2015.

481 Hailu, K., Fechete, R., Demco, D. E., Blümich, B.: Segmental anisotropy in strained elastomers detected with a
482   portable NMR scanner, Solid State Nucl. Magn. Reson. 22, 327–343, 2002.

483 Haken, R., Blümich, B.: Anisotropy in Tendon Investigated in Vivo by a Portable NMR Scanner, the NMR-
484   MOUSE, J. Magn. Reson. 144, 195–199, 2000.

485 Hürlimann, M. D., Griffin, D. D.: Spin Dynamics of Car-Purcell-Meiboom-Gill-like sequences in grossly
486   inhomogeneous B_0 and B_1 fields and applications to NMR well logging, J. Magn. Reson. 143, 120–135,
487   2000.

488 Jackson J. A., Burnett, L. J., Harmon, J. F.: Remote (inside-out) NMR. III. Detection of nuclear magnetic
489   resonance in a remotely produced region of homogeneous magnetic field, J. Magn. Reson. 41, 411–421,
490   1980.

491 Johns, M. L., Fridjohnsson, E. O., Vogt, J. J., Haber, A., eds.: Mobile NMR and MRI: Developments and
492   Applications, Royal. Soc. Chem., Cambridge, 2016.

493 Kern, S., Wander, L., Meyer, K., et al.: Flexible automation with compact NMR spectroscopy for continuous
494   production of pharmaceuticals, Anal. Bioanal. Chem. 411, 3037–3046 (2019).

495 Keschenau, P. R., Klingel, H., Reuter, S., et al.: Evaluation of the NMR-MOUSE as a new method for continuous
496   functional monitoring of the small intestine during different perfusion states in a porcine model, PLOS ONE
497   0206697, 1–17, 2018.

498 Kleinberg, R. L., Jackson, J.A.: An Introduction to the History of NMR Well Logging, Concepts Magn. Reson.
499   13, 340–342, 2001.

500 Nordon, A., McGill, C. A., Littlejohn, D.: Process NMR spectrometry, Analyst 126, 260–272, 2001.

501 Oligschläger D., Lehmkuhl, S., Watzlaw, J., et al.: Miniaturized multi-coil arrays for functional planar imaging
502   with a single-sided NMR sensor, J. Magn. Reson. 254–18, 2015.

503 Oligschläger, D., Glöggler, S., Watzlaw, J., et al.: A Miniaturized NMR-MOUSE with a High Magnetic Field
504   Gradient (Mini-MOUSE), Appl. Magn. Reson. 46, 181–202, 2015.

505 Oligschläger, D., Kupferschläger, K., Poschadel, T., Watzlaw, J., Blümich, B.: Miniature mobile NMR sensors
506   for material testing and moisture-monitoring, Diffusion Fundamentals 22, 1–25, 2014.

507 Olmi, R., Bini, M., Ignesti, A., et al.: Diagnostics and monitoring of frescoes using evanescent-field
508   dielectrometry, Meas. Sci. Technol. 17, 2281–2288, 2006.

509 Perlo, J., Casanova, F., Blümich, B.: Ex situ NMR in highly homogeneous fields: [1]H spectroscopy, Science 315,
510   1110–1112, 2006.

511 Perlo, J., Casanova, F., Blümich, B.: Profiles with microscopic resolution by single-sided NMR, J. Magn. Reson.
512   176, 64–70, 2005.

513 Perlo, J., Demas, V., Casanova, F., et al.: High-resolution NMR spectroscopy with a portable single-sided sensor,
514   Science 308, 1229, 2005.

515 Prati, S., Sciutto, G., Volpi, F., et. al.: Cleaning oil paintings: NMR relaxometry and SPME to evaluate the effects
516   of green solvents and innovative green gels, N. J. Chem. 43, 8229–8238, 2019.

517 Presciutti, F., Perlo, J., Casanova, F., et al.: Noninvasive nuclear magnetic resonance profiling of painting layers,
518   Appl. Phys. Lett. 93, 033505, 2008.

519 Proietti, N., Capitani, D., Rossi, E., Cozzolino, S., Segre, A. L.: Unilateral NMR study of a XVI century wall
520   painted, J. Magn. Reson. 186, 311–318, 2007.

521 Rehorn, C., Blümich, B.: Cultural Heritage Studies with Mobile NMR, Angew. Chem. Int. Ed. Eng. 57, 7304–
522   7312, 2018.

523 Rehorn, C., Kehlet, C., Del Federico, E., et al.: Automatizing the comparison of NMR depth profiles, Strain 54,
524   e12254, 2018.

525 Rühli, F., Böni, T., Perlo, J., et al.: Non-invasive spatial tissue discrimination in ancient mummies and bones in
526   situ by portable nuclear magnetic resonance, J. Cultural Heritage 8, 257–263, 2007.

527 Saalwächter, K., Microstructure and dynamics of elastomers as studied by advanced low-resolution NMR
528   methods, Rubber Chem. Tech. 85, 350–386, 2012.

529 Segre, A. L., Blümich, B.: Progetto 'MOUSE': Risonanza magnetica per i beni culturali, Ricerca & Futuro 25, 34–
530   36, 2002.

531 Van Landeghem, M., Danieli, E., Perlo, J., Blümich, B., Casanova, F.: Low-gradient single-sided NMR sensor for
532   one-shot profiling of human skin, J. Magn. Reson. 215, 74–84, 2012.

533 van Putte, K., van den Enden, J.: Fully automated determination of solid fat content by pulsed NMR, J. Am. Oil
534   Chem. Soc. 51 316–320, 1974.

535 Varian, R. H.: Apparatus and Method for Identifying Substances, US patent 2,651,490, filed 3 January 1952.

536 Watzlaw, J., Glöggler, S., Blümich, B., Mokwa, W., Schnakenberg, U.: Stacked planar micro coils for single-sided
537   NMR applications, J. Magn. Reson. 230, 176–185, 2013.

538 Woessner, D. E.: The Early Days of NMR in the Southwest, Concepts Magn. Reson. 13, 77–102, 2001.

539 Zalesskiy, S.S., Danieli, E., Blümich, B., Ananikov, V. P.: Miniaturization of NMR systems: desktop
540   spectrometers, microcoil spectroscopy, and "NMR on a chip" for chemistry, biochemistry, and industry,
541   Chem. Rev. 114, 5641–5694 (2014).